SOME DYNAMIC ASPECTS FOR THE DESIGN OF HIGH-SPEED TRACK

Coenraad Esveld

Delft University of Technology / Esveld Consulting Services

Abstract

TU Delft developed new force-based geometrical standards for rail welds on behalf of the Dutch Rail Infra Manager ProRail. Previous standards were based on the principle of maximum vertical and horizontal tolerances, as is worldwide common practice. However, this approach does not account for the geometrical shape of the weld. In this way, the relation with the dynamic wheel-rail contact forces and stresses is disregarded, whereas these forces determine the rate of track deterioration.
In this paper a theoretical model is presented to translate dynamic wheel-rail contact forces into the 1st derivative of the weld geometry. Intervention values depending on the line section speed are presented. Measurement and simulation results show good correspondence with the theory. The new assessment method requires the application of digital straightedges like the RAILPROF instead of steel straightedges, in order to obtain the weld quality index according to the new standards.

In the second part the dynamic analysis of the track structure is discussed. On top of this low frequency response the high-frequency impact response due to welds should be superimposed. This is primarily important in the area near the wheal rail interface, as the high-frequency loads damp out quickly.

High frequency loads near welds

Delft University of Technology has developed new technical standards for the geometrical deviations of metallurgic rail welds in the Netherlands, in cooperation with the Dutch Rail Infra Manager ProRail [1,2]. Like in all norms worldwide, the previous Dutch standards for vertical weld geometry were based on the principle of deviations of the vertical geometry measured as a versine on a 1-meter base.
In this approach, only the maximum value of the longitudinal rail surface irregularity is decisive, whereas the geometrical shape has no significance. However, this shape has a direct relation to dynamic wheel-rail contact forces, which may not be neglected: the power spectrum of the dynamic wheel-rail contact forces determines the rate of track deterioration and the degradation of vehicle and track components.
Secondly, in an approach based on geometrical deviations, the train velocity has no influence. It is clear however, that the contact forces depend on the train speed.
In order to tackle these shortcomings a method was developed to evaluate the 'dynamic quality' of the weld geometry in relation to the train speed.

Standardization and assessment based on first spatial derivatives

In [1,3], a comparative study has been made for an assessment method based on 0^{th}, 1^{st} and 2^{nd} spatial derivatives of the measured weld. It has been concluded that an approach based on the 1^{st} derivative had the best performance, the 2^{nd} derivative being extremely sensitive to short indentations, and not very sensitive to irregularities with a longer wavelength. The following values, proposed by TU Delft [2] were adopted in the Dutch standards (2005):

- $v \leq 40$ km/h 3.2 mrad
- $40 \leq v \leq 80$ km/h: 2.4 mrad
- $80 \leq v \leq 140$ km/h: 1.8 mrad (1)
- $140 \leq v \leq 200$ km/h: 0.9 mrad
- $200 \leq v \leq 300$ km/h: 0.7 mrad

The last value, for high-speed lines, corresponds to the quality of new rails. The value has been determined by analysis of a sample of 100 rail segments of 1 m, where 0.7 mrad is found as the upper bound of the 95% reliability interval.
For assessment purposes, the weld Quality Index (QI) is introduced as the dimensionless ratio of the actual value for the 1st derivative of the weld geometry to the speed-dependent norm value. A value smaller than or equal to 1 implies acceptance, whereas a value larger than 1 leads to rejection. Or, in formula, for a given train speed *v*:

$$\mathrm{QI} = \frac{\left|\frac{dz(x)}{dx}\right|_{\max,actual}}{\frac{dz}{dx}_{norm}} \quad (\leq 1\text{: acceptance; } > 1\text{: rejection}) \tag{2}$$

The relation between the QI and the wheel-rail contact force

The geometry of rail welds is commonly measured with a digital straightedge with 1 m basis and a sample interval of 5 mm. For assessment purposes, the signal is averaged, with an increase of the sample interval to 25 mm [2]. A range of wavelengths in a measurement signal from 0.1 m up to 2 m ensues. Combining this interval with a velocity range for conventional passenger trains and freight trains of 80-140 km/h, a corresponding frequency-range 10-400 Hz can be established. Generally, in this frequency-range several stiffnesses and masses play a role in train-track-dynamics. The most important masses are the unsprung wheelset mass and the equivalent track mass, whereas the primary suspension stiffness, the wheel-rail Hertzian contact stiffness and the equivalent track stiffness are the most important stiffnesses. For each frequency a certain mass in combination with a related stiffness plays a dominating role and determines the magnitude of wheel-rail contact forces. Assuming a quasi-static response for the dominating mass (*M*) – stiffness (*K*) combination, disturbed by the weld irregularity as a function of the longitudinal coordinate *z*(*x*) moving at train speed *v*, the dynamic component of the wheel-rail contact force is equal to the inertia force originating from the mass *M* which follows the vertical irregularity [4], or, according to Newton:

$$F_{dyn}(t) = \alpha m_e \ddot{z}(t) = \alpha m_e \frac{d}{dt}\left(\frac{dz(t)}{dt}\right) \text{ where } m_e = \frac{ML_n}{L_0} \tag{3}$$

In this expression, m_e represents a frequency-dependent equivalent mass, determined as the dominant mass in the wheel-rail system multiplied with the wavelength. L_0 is a reference wavelength.
Each measurement signal of a rail weld in longitudinal direction $z(x)$ can be decomposed, using DFT-techniques, into a finite number of harmonics:

$$z(x) = \sum_{n=1}^{N} z_n \sin\frac{2\pi x}{L_n} \quad \rightarrow \quad z(t) = \sum_{n=1}^{N} z_n \sin\frac{2\pi v t}{L_n} \tag{4}$$

In the following, one single harmonic is considered ($N = 1$). The final result can be easily extended for larger *N*. Then, substitution of (3) and (4), respectively, yields:

$$F_{dyn}(t) = \alpha m_e \frac{d}{dt}\left(z_1 \frac{2\pi v}{L_1}\cos\frac{2\pi v t}{L_1}\right) = \alpha 2\pi v \frac{M}{L_0}\frac{d}{dt}\left(z_1 \cos\frac{2\pi v t}{L_1}\right) \tag{5}$$

Via $x = vt$ follows, in the space domain:

$$F_{dyn}(x) = \alpha 2\pi v^2 \frac{M}{L_0}\frac{d}{dx}\left(z_1 \cos\frac{2\pi x}{L_1}\right) \tag{6}$$

Since only the maximum value of the dynamic force is of interest, and not its position, the cosine terms in the above expression may be replaced by sine terms, as in the original expression (4), yielding:

$$F_{dyn,\max} = \alpha 2\pi v^2 \frac{M}{L_0}\left|\frac{dz(x)}{dx}\right|_{\max}, \text{ or, alternatively: } F_{dyn,\max} = \beta \frac{Mv^2}{L_0}\left|\frac{dz(x)}{dx}\right|_{\max} \quad (7)$$

Thus, the maximum dynamic component of the wheel-rail contact force, corresponding to a specific sampled weld, is expressed in terms of its maximum spatial first derivative, or, equivalently, the QI:

$$F_{dyn,\max} = \beta \frac{Mv^2}{L_0}\frac{dz}{dx}_{norm} \cdot \mathrm{QI} \quad (8)$$

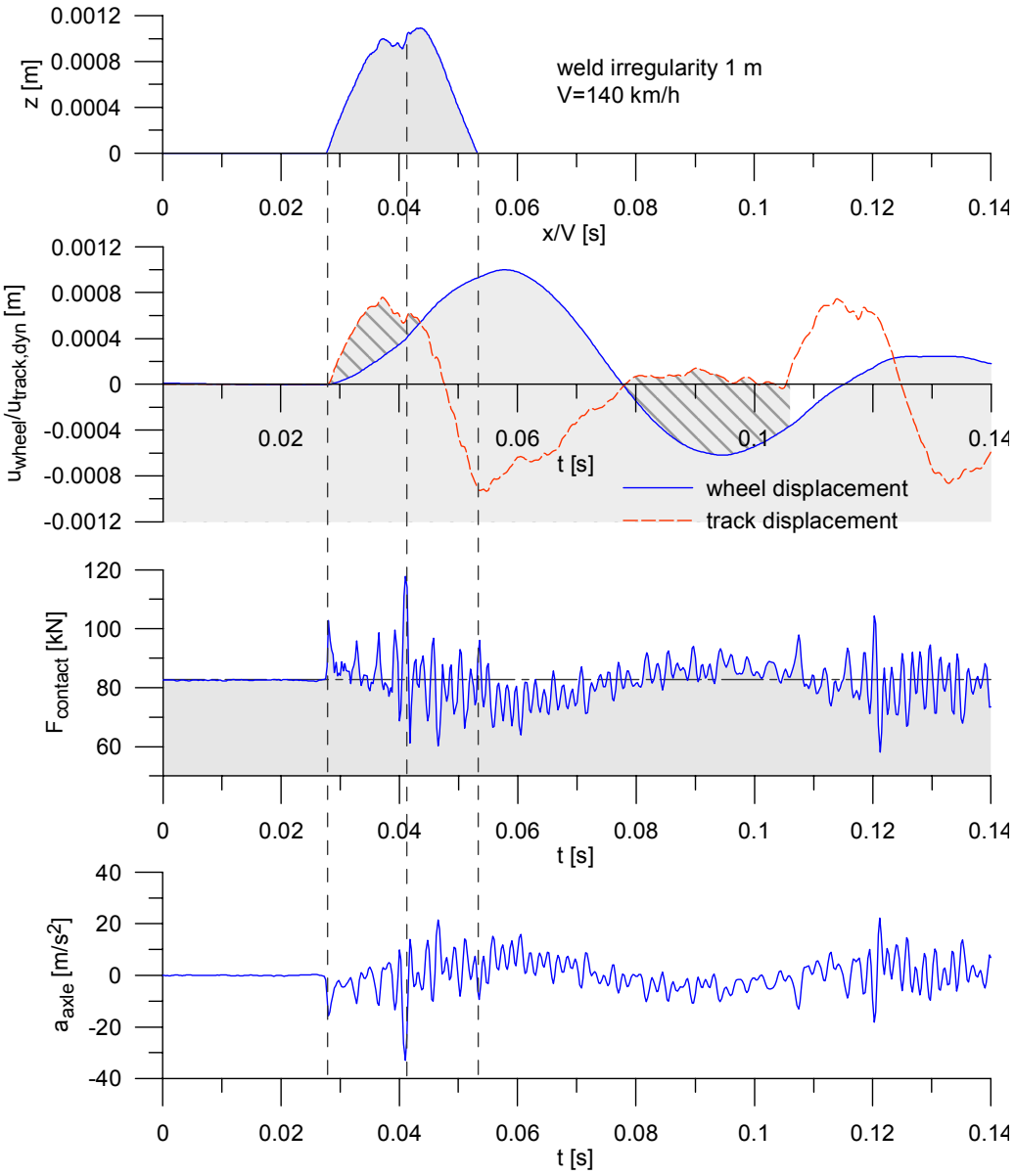

Figure 1: Dynamic response of the wheel-rail system at a rail weld surface irregularity

Figure 1 shows the dynamic response of the wheel-rail system to a measured rail weld irregularity, calculated with the finite element package DARTS-NL [5], where representative values for the track parameters have been adopted in the calculation. The train speed has been taken as 140 km/u. The graphs show the measured rail surface irregularity *z*, the dynamic part of the rail deflection, in a fixed coordinate system with origin at the centre of the irregularity and defined downward in positive direction, the wheel displacement in a reference frame moving along with the wheel and defined upward in positive direction,

the contact force between wheel and rail, and the axle box acceleration of the considered wheel, where all parameters are a function of time. The repetitive pattern in the rail deflection is due to the passage of the second axle in the bogie.
In Figure 1, it can be observed that the maximum dynamic contact force is determined by the irregularities with the shortest length-scale. However, the corresponding force peaks are rather narrow, and the corresponding energy amount is rather small. The highest energy of the dynamic contact force is contained in the 'carrier frequency', which can be clearly observed. This carrier frequency is related to the instantaneous reaction of the track mass and the delayed reaction of the wheel mass to the irregularity. This phenomenon (indicated by the hatched areas in Figure 1) is responsible for the occurrence of P_1 and P_2 forces respectively, as has been established in [4] for welded rail connections.

The dynamic wheel-rail response at welds; numerical and experimental results

In order to validate the relationship (8) between the QI and the dynamic contact forces, measurements have been carried out of the weld geometry on the Dutch network. This geometry has been registered for 239 welds. Subsequently, the corresponding dynamic contact forces have been calculated using the FEM-package DARTS-NL [5]. Figure 2 shows the cumulative distribution of 3 series of measurements carried out with the RAILPROF on the ProRail network. The welds passing the 1.8 mrad criterion for 140 km/h line speed varies from 31% to 81 %. This reveals that the weld geometry condition on ProRail is rather poor.
In Figure 3 the cumulative distribution function of 239 weld from the earlier mentioned population is displayed and in this case 46% of the population satisfies the norm of 1.8 mrad at 140 km/h.

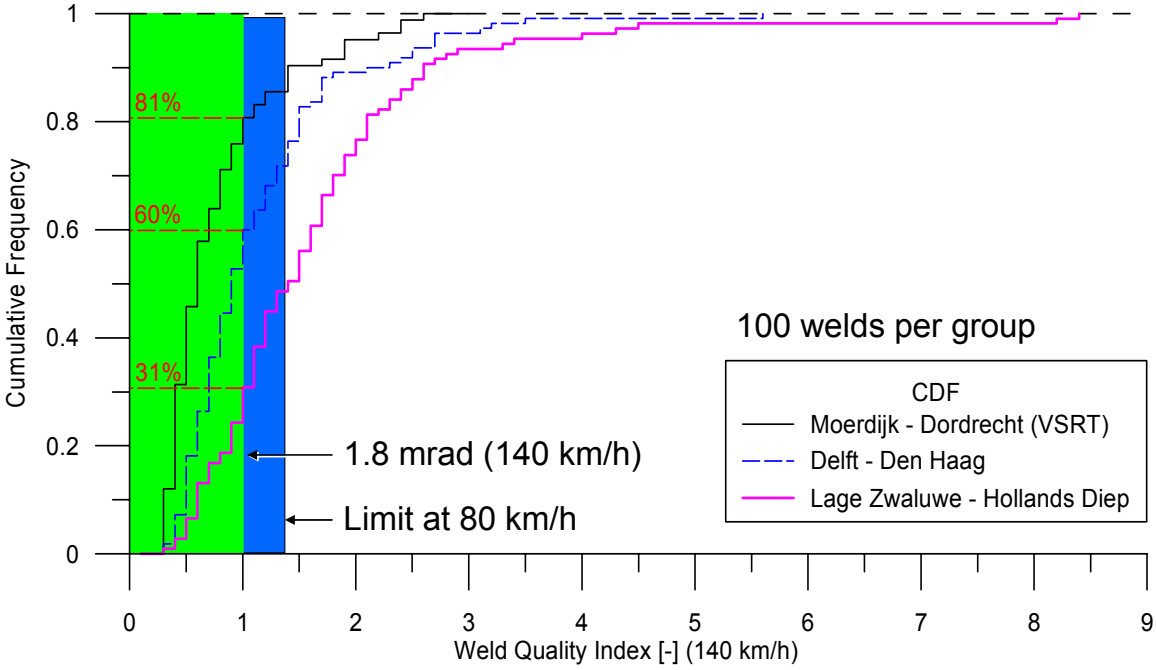

Figure 2: Cumulative distribution of 3 set of weld geometry obtained by RAILPROF measurements

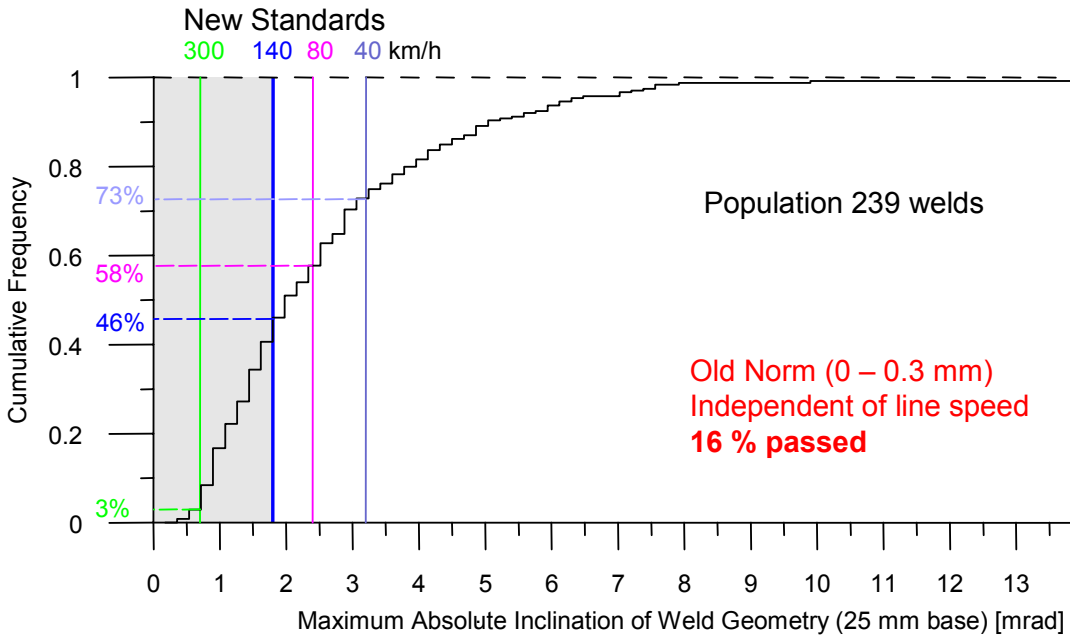

Figure 3: Cumulative frequency distribution of the set of weld measurements, used in the simulations

Figure 4 shows the maximum dynamic contact forces as a function of both the vertical deviation and the maximum slope of the weld (which is directly related to the QI), where the speed is chosen as 140 km/h. The following parameter values have been adopted in the simulations: a wheel mass (half un-sprung mass) of 970 kg; a sleeper mass of 300 kg; UIC 54 rail; a primary suspension stiffness of 1.8e6 N/m (per wheel); a rail-pad stiffness of 1.2e9 N/m and a ballast stiffness of 30e6 N/m per sleeper, where the latter value is rather small, to account for the generally bad compaction of the ballast underneath the sleepers close to the irregularity. A non-linear Hertzian contact model has been used.
In both graphs in Figure 4, a linear fit, calculated with a least-squares method, is displayed. The value of R^2 is a measure for the goodness of fit, 0 indicating a zero correlation and 1 a perfect correlation. It is clear that the correlation between maximum dynamic contact forces and the maximum slope is much better (0.91) than the correlation with the versine, which is close to zero. The scatter is due to the assumptions in the derivation of (7).

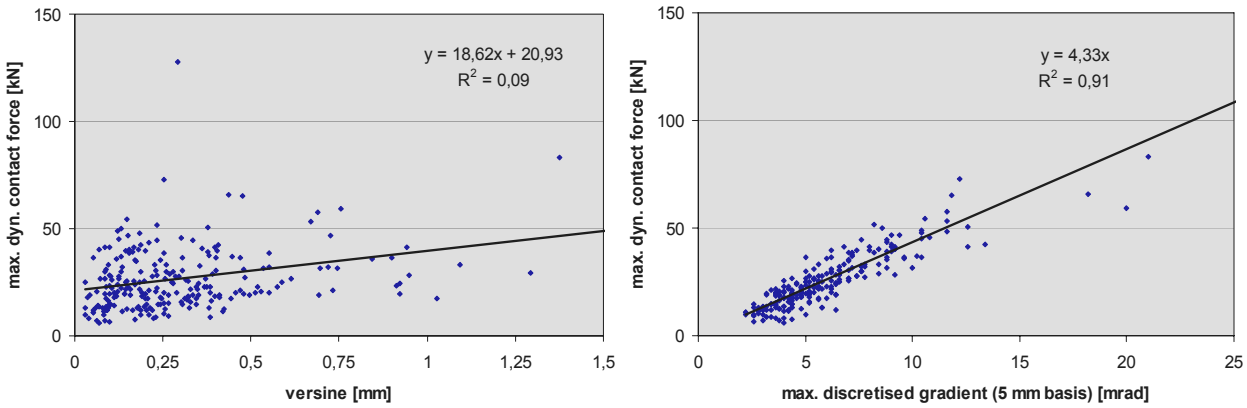

Figure 4: Numerical simulation results of the dynamic contact force at rail welds; maximum dynamic force as a function of the maximum versine and the QI (140 km/h).

Figure 4 shows dynamic contact forces generally ranging from 0 to 100 kN. The static axle load has been taken as 82 kN. Therefore, the following dynamic amplifications are found for the contact forces:

$$\varphi = 1 + \frac{F_{dyn}}{F_{stat}} < 1 + \frac{100}{82} \approx 2.2 \qquad (9)$$

Generally speaking, the DAF for the axle loads will be lower than 2 at 140 km/h.

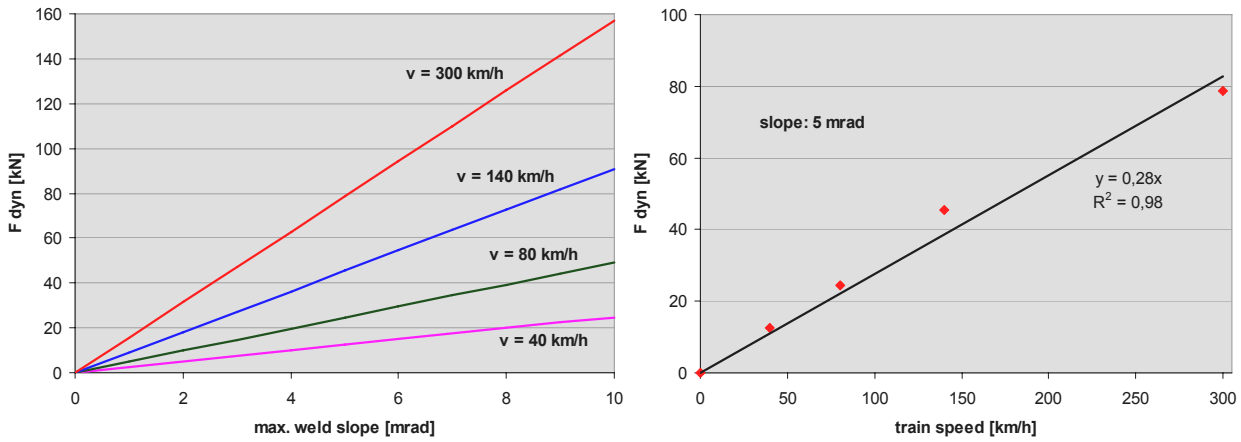

Figure 5: Numerical simulation results of the dynamic wheel-rail force versus the discrete weld slope (linear fits) at different velocities; dynamic force versus train velocity for a given slope

Figure 5 shows simulation results of the maximum dynamic wheel-rail contact forces at different velocities as a function of the discrete slope of the weld geometry; for each velocity a linear fit is depicted. At the right, this force is shown as a function of the train velocity for a given maximum slope. The increase, which is more than linear for velocities up to 140 km/h, and less than linear between 140 and 300 km/h, can be well approximated with a linear fit.

In Figure 6, measurement results are shown of the dynamic contact forces between wheel and rail for different weld geometries which have been ground into the rail surface, for a train velocity of 140 km/h. The peak forces, which are shown per train, have been determined as the average value for all axles of the passing train. It is obvious that the correlation of the maximum contact forces with the QI is much better than the correlation with the versines. The lines corresponding to the standard deviations are also shown in Figure 6. The relatively large scatter is partly due to the fact that not all conditions, except for the weld geometry, have been constant during the measurements.

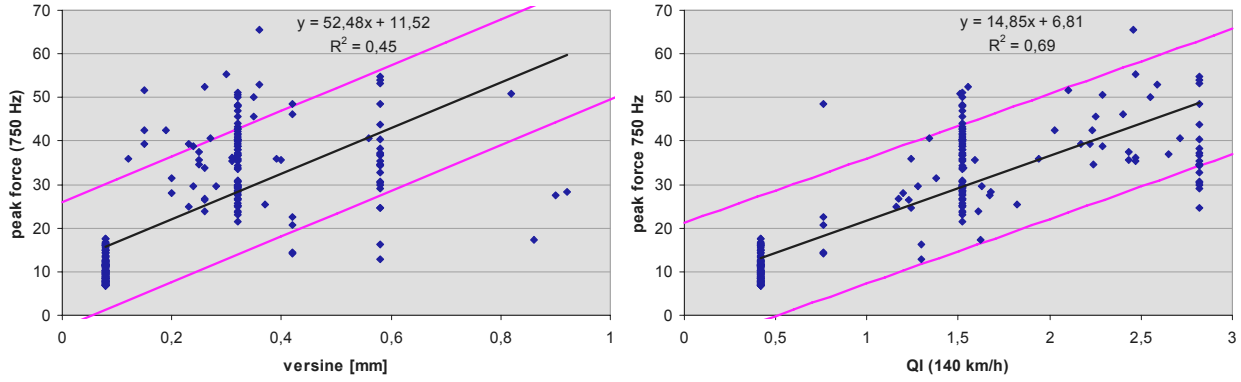

Figure 6: Measurement results of the dynamic contact force at rail welds; maximum dynamic force in a frequency band up to 750 Hz as a function of the maximum versine and the QI (140 km/h).

Figure 7 shows the dynamic amplification of the static axle load, averaged per train. The cut-off frequency has been chosen as 350 and 750 Hz respectively. The trend with the QI can be approximated as linear. The magnitude of the DAF is generally below 2, as has been found from the simulations.

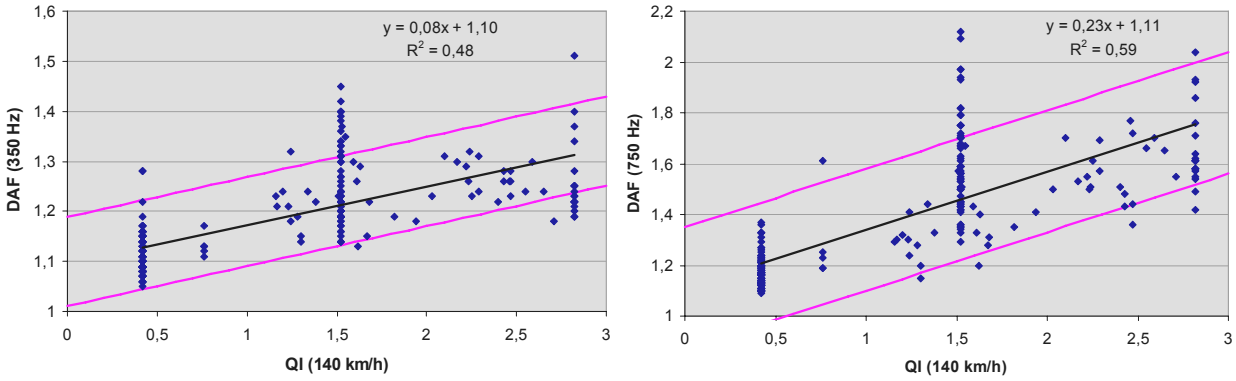

Figure 7: Measurement results of the dynamic contact force at rail welds; dynamic amplification of the static axle load in a frequency band up to 350 and 750 Hz respectively as a function of the QI (140 km/h).

Weld assessment according to the new method in practice

In practice, the new geometrical assessment of a weld, in vertical direction, is made according to the following steps:

1. The weld is measured, both vertically and laterally, with a 1 m digital straightedge with a sampling interval of 5 mm.
2. In vertical direction, the software of the straightedge filters out irregularities with length-scale smaller than 25 mm, calculates the 1st derivative of the filtered geometry, and divides the discrete values of the first derivative by the speed dependent norm (1), after which the maximum is determined. In this way the QI of the weld is obtained.
3. The geometry itself is plotted, together with the absolute value of the normalized first derivative, on the graphical display (which may be remote, using a PDA (Figure 8)) so that the welding crew can immediately see the result of their work. If the QI is larger than 1 the weld is rejected and additional grinding is required; if the QI is smaller than 1, the weld is accepted. For example, the weld in Figure 2 (right) has a QI of 1.06, and should be ground in the middle before acceptance.

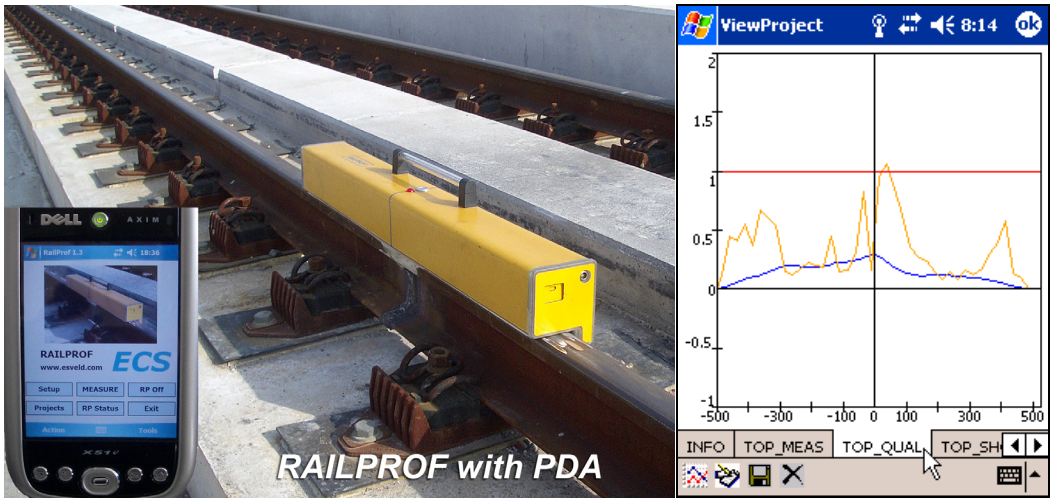

Figure 8: Digital straightedge (Railprof [4]) with PDA and software for the assessment of a measured weld

Testing and certification of measuring equipment

The QI approach requires a high measuring accuracy of at least 0.18 mrad for 140 km/h and 0.07 mrad for 300 km/h. It is therefore absolutely necessary to have reliable testing and certification procedures, taking into consideration influences of rust, dirt moisture and temperature. Especially capacitive measurement techniques are very susceptible for these influences.

ProRail opted for a 1.5 m reference rail, milled straightly, with in the center a cosine shaped indentation of 0.3 mm and a length of 500 mm, corresponding to a QI = 1.034.

Conclusions on weld geometry standards

1. The theory developed on basis of the first derivative provides a practical tool to assess the geometrical quality of rail welds from a point of view of dynamic wheel-rail contact forces and track deterioration.
2. Simulations and measurements of maximum dynamic contact forces at rail welds show a much better correlation with the QI than with the versine.
3. For a conventional passenger train speed of 140 km/h, dynamic amplifications of the axle load are found which are generally smaller than 2.
4. The proposed method is uniform and easy to implement in practice, using digital straightedges.

Dynamic analysis of the track structure (long waves).

At TU Delft various dynamic analyses of structures for high-speed lines have been made with the finite element model DARTS_NL [6]. This program had been specially developed for the dynamic analysis of the vertical interaction between vehicle and track structure. This is at low frequencies up to about 50 Hz. As an example the dynamic analysis for a special bridge type of slab track supported by piles (Figure 9) will be shown. The analyses have been performed for the Thalys and the ICE3M at speeds of 40, 65 and 90 m/s.

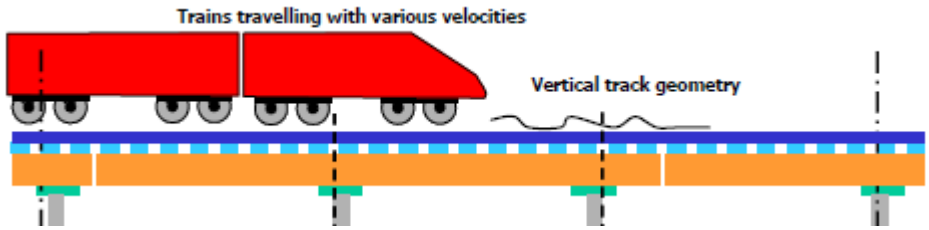

Figure 9 Schematic representation of the FE model used in the dynamic analysis

The output basically consists of:

- Vertical accelerations of the train coaches for the passenger's comfort estimation
- Vertical wheel-rail interaction forces for estimation of the dynamic amplification factors
- Accelerations, forces and bending moments of the concrete slab

The numerical simulations were performed for the time frames from 3.5 to 7.5 seconds (depending on the train velocity) with the time step of 0.5 milliseconds. Within these time frames the modeled trains travel approximately 520 meters so that in each simulation a train passes at least once a selected part of the track. The vertical rail level geometry file used in the dynamic simulations was composed from a short wave [3-25m] profile obtained from a measurement train and a long wave profile which was constructed artificially. The geometrical properties of the composed vertical rail level geometry profile used in the simulations for various wave bands are collected in Tab. 1. The PSD function is represented in Figure 10 and the spatial geometry in Figure 11.

Waveband	Level	
	Umax [mm]	**σ [mm]**
3 - 25 m	4.6058	1.0296
25 - 70 m	3.8831	1.3849
70 - 180 m	6.4151	2.7211

Tab. 1 Maximum amplitude (Umax) and standard deviation (σ) of the vertical rail level geometry profile used in the simulations

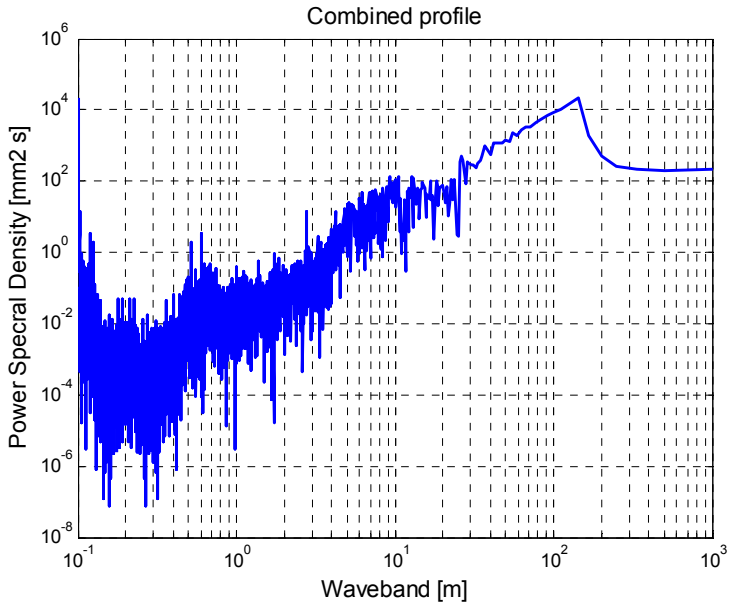

Figure 10 Total vertical geometry versus frequency (PSD function)

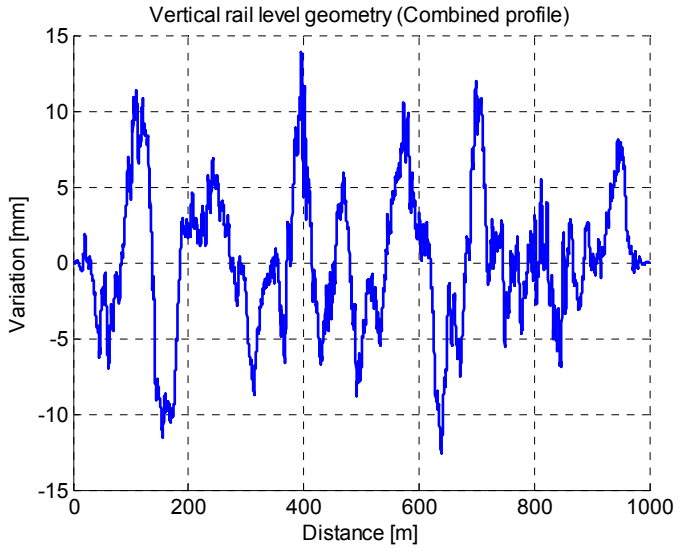

Figure 11. Total vertical geometry versus space.

Vertical accelerations

Accelerations experienced by passengers in the train bodies should not exceed their limit values within the time frame to avoid being considered as 'uncomfortable'. These limits are defined in terms of the passenger's comfort according to the UIC 513 standard, quality level 2. In the simulations, only vertical accelerations were taken into consideration, whereas the UIC standard uses weighted three-dimensional accelerations. With some approximations a link between the vertical accelerations obtained from the simulations and the UIC standard could been established. According to the calculations the obtained limit has been set to 0.38 m/s2 standard deviation for mechanical vibrations in vertical direction in the train bodies at any position.
The maximum train accelerations with the normal quality (σ[3-25 m]≈ 1.0 mm) was 0.26 for the Thalys and 0.16 for the ICM3M. For the rough rail geometry (σ[3-25 m]≈ 1.5 mm) these values were respectively 0.39 and 0.24, always at 90 m/s.

Wheel-rail interaction forces

Wheel-rail interaction forces corresponding to all wheels of the running trains are reported here. Instead of maximum interaction forces, 1.96 times the standard deviation is calculated in the simulated time frames, which corresponds to the 95% coverage in the normal distribution (2σ). This value summed with the nominal (static) wheel force is then considered relative to the nominal wheel force, so that the dynamic amplification factor (DAF) is calculated.

According to the Eurocode (ENV 1991-3:1995 6.4.3.2) the following DAF limits should be adhered to: a limit of 1.67 for a "carefully maintained track" and a limit 2.00 for a "track with standard maintenance". Similar limits have been established in the HSL-Zuid norms (HSL 600E 3.2.3). The numerical results show the maximum value at 40 m/s, being for both train types 1.7 for the normal rail and 2.5 for the rough rail. The results of the simulations have emphasized again the importance of maintenance of the vertical rail geometry on the required level. The value of 2.5 can be lowered by allowing less deviation in the geometry, or by increasing the stiffness of the structure.

Forces and bending moments in the structure

Bending moments in the slab are related to the maximum wheel force and the wheel spacing. Maximum bending moments occur directly below the passing wheel, minimum moments just in front, or behind the wheels. The maximum dynamic bending moment of the concrete slab obtained here are found to be -309 kNm which value satisfies the requirements of the German DIN FB 102.

Conclusions on low frequency dynamics

The results of the numerical simulations have demonstrated that the quality of rail geometry has a great influence on the dynamic responses such as vehicle accelerations and wheel-rail contact forces. In fact the maximum value of the geometry is also the maximum which can be allowed in the track, if these maximum values found are at the admissible limit. Also the influence of the slab design on the dynamic responses is rather strong. Normally a greater stiffness results is less amplification.

References

[1] M.J.M.M. Steenbergen, C. Esveld. *Proposal for new rail weld geometry standards* (in Dutch), report 7-04-220-7, ISSN 0169-9288, TU Delft, Delft, (2004).
[2] M.J.M.M. Steenbergen, C. Esveld, R.P.B.J. Dollevoet. "New Dutch Assessment of Rail Welding Geometry", *European Railway Review*, Issue 1, (2005).
[3] C. Esveld, M.J.M.M. Steenbergen. "Force-Based Assessment of Weld Geometry", *Proc. 8th International Heavy Haul Conference*, Rio de Janeiro, (2005).
[4] M.J.M.M. Steenbergen, C. Esveld. "On Rail Weld Geometry and Assessment Concepts", *Proc. Inst. Mech. Engs. Part F: J. of Rail and Rapid Transit*, in press (2006).
[5] www.esveld.com
[6] C. Esveld. "Modern Railway Track", MRT-Productions, www.esveld.com, ISBN 90-800324-3-3, (2001)